NACA RM L57D24

NACA

RESEARCH MEMORANDUM

THE SINE-COSINE METHOD FOR REDUCING THE INTERFERENCE PRESSURE DRAG OF SWEPTBACK WINGS

By Maxime A. Faget

Langley Aeronautical Laboratory
Langley Field, Va.

NATIONAL ADVISORY COMMITTEE
FOR AERONAUTICS

WASHINGTON
July 2, 1957
Declassified January 12, 1961

NATIONAL ADVISORY COMMITTEE FOR AERONAUTICS

RESEARCH MEMORANDUM

THE SINE-COSINE METHOD FOR REDUCING THE INTERFERENCE PRESSURE DRAG OF SWEPTBACK WINGS

By Maxime A. Faget

SUMMARY

A design procedure for reducing the interference pressure drag of the root and tips of sweptback wings is described. This is accomplished by modifying the fuselage cross-sectional area in the vicinity of the wing root and by adding specifically shaped stores at the wing tips in order that the rate of change of cross-sectional area of these bodies is proportional to the wing-section thickness. The constant of proportionality is the product of the sine and cosine of the local angle of sweepback. This method, called the sine-cosine method, was arrived at by using one-dimensional incompressible flow relations to obtain average spanwise flow deflections over the wing. Experimental and theoretical pressure-drag values from Mach number 0.9 to 1.35 for configurations designed by this method were compared with the values of two similar configurations designed by the transonic and supersonic area-rule methods. Although the sine-cosine configuration with wing-tip stores had more usable volume than the area-rule configurations, it was found to have lower drag than the transonic area-rule configuration and approximately the same drag as the supersonic area-rule configuration.

INTRODUCTION

The transonic-drag coefficient of sweptback wings of finite span is considerably greater than the theoretical values for corresponding yawed wings of infinite span. This is caused by the interference from the flow field of one panel upon the other at the center and from the changes in the flow field at the tips. Methods have been proposed for alleviation of the interference at the center by shaping the body (refs. 1 and 2), and experimental results have indicated that considerable reduction in the interference drag may be obtained by these methods (refs. 3, 4, 5, and 6). Similarly, interference drag reductions were obtained by indenting the sides of the body to conform with the predicted surface streamline over the wing. (See refs. 7, 8, 9, and 10.)

The transonic area rule (ref. 11) has demonstrated the importance of the cross-sectional area variation in the alleviation of interference effects. Therefore, it was considered likely that modifying the fuselage cross-sectional area along the wing root chord to allow for the inward displacement of the natural stream flow (as in the case of the infinitely yawed wing) might be sufficient to alleviate the wing-root interference. Similarly, the interference produced by the flow discontinuity at the wing tips could be alleviated by small shapes at the tips. A simple method approximating the lateral area displacement of the streamlines was devised, and experimental tests of the effectiveness of this scheme were made for a Mach number range from 0.9 to 1.35 by use of 45° swept-wing rocket-powered models.

SYMBOLS

A	cross-sectional area normal to body axis, sq in.
a	acceleration, ft/sec^2
C_D	drag coefficient based on S
ΔC_D	pressure-drag coefficient based on S
D	vertical distance between imaginary planes channeling the flow over the wing
g	acceleration due to gravity, 32.2 ft/sec^2
L	length of body, in.
q	free-stream dynamic pressure, lb/sq ft
R	Reynolds number (based on wing mean aerodynamic chord)
r	body radius, in.
S	wing area, leading and trailing edge extended to fuselage center line, sq ft
t	local wing thickness
V	local stream velocity
V_N	component of local stream velocity normal to wing leading edge

V_T component of local stream velocity tangential to wing leading edge

V_X component of local velocity parallel to flight path

V_Y component of local velocity normal to flight path and parallel to wing plane

W weight, lb

X distance measured from nose, rearward along body axis

Y distance from body axis to body side

γ elevation angle of flight path

Λ angle of sweepback

APPROXIMATION OF AREA DISPLACEMENT BY STREAM SHEETS

The flow over a yawed wing of infinite span may be considered to consist of a vector normal to the wing leading edge and a vector tangential to the wing leading edge. The tangential velocity vector will remain unchanged as the air passes over the wing; whereas, the normal velocity vector is changed in magnitude as the flow is accelerated over the airfoil. The amount of change in magnitude of this vector is of course different at various distances away from the wing surfaces as well as along the chord. By recombining the tangential and normal vectors in various regions of the flow which are affected by the airfoil, a resultant vector is obtained which describes the local direction of the flow.

An acceleration of the flow over the wing results in an increase in magnitude of the vector normal to the wing leading edge and thus the flow is turned inwardly. Similarly, where the flow is decelerated it is turned outwardly. A set of streamlines orignating as a vertical plane oriented along the axis of flight (the wing considered to be in the horizontal plane) makes up the stream sheet of interest to this analysis. As this stream sheet passes over and under the wing, it is first turned inwardly and then outwardly, the portion closest to the wing being deflected the most.

When the air is allowed to pass freely over the yawed wing, the Mach number normal to the leading edge determines the extent of compressibility effects on the flow. Therefore, transonic free-stream

Mach numbers should be obtainable with negligible drag rise. The usual sweptback wing of finite span will not ordinarily achieve this flow condition because the stream sheet of both wings is deflected toward the center and, as transonic speeds are approached, the stream flow caught between these stream sheets is unable to accommodate the area reduction required. Accordingly, one approach to reducing the drag at transonic speeds is to estimate the inward area displacement of the stream sheets and then tailor the cross-sectional area of the fuselage in the vicinity of the wing root to accommodate this displacement. Similarly, at the wing tips the necessary inward displacement of the stream sheets may be created by small properly shaped bodies.

In order to determine exactly the displacement of the stream sheet, it would be necessary to determine the velocity profile that exists for some distance outward over the wing at every wing station. However, this inward displacement may be approximated by assuming the following simplifying conditions: (1) the flow is incompressible (2) the normal velocity does not vary at any one station with distance outward from the wing surface to the limit of the stream sheet under consideration (that is, one-dimensional flow), and (3) the spanwise velocity component is constant.

Consider that the flow is confined between a pair of parallel planes above and below the wing. The distance D between these planes is shown in the following sketch:

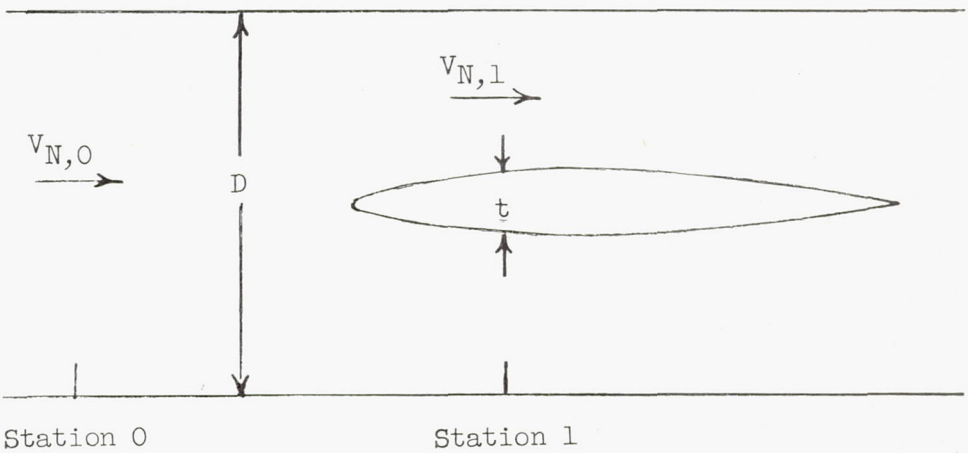

At station 0 the normal velocity is $V_{N,0}$ and at station 1 the normal velocity will be

$$V_{N,1} = V_{N,0} \frac{D}{D - t} \tag{1}$$

The increase in velocity is therefore

$$\Delta V_N = V_{N,0}\left(\frac{D}{D - t} - 1\right) \tag{2}$$

$$\Delta V_N = V_{N,0}\left(\frac{t}{D - t}\right) \tag{3}$$

The magnitude of sidewise area displacement by this velocity increase is next determined. This is illustrated by the following vector diagram:

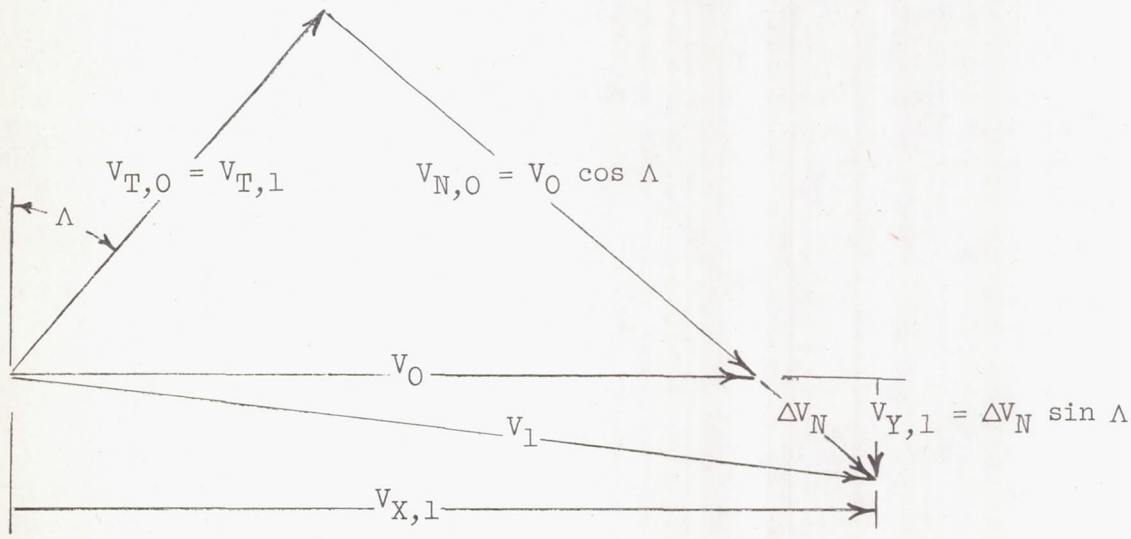

where

$$\frac{dA}{dX} = \frac{V_{Y,1}D}{V_{X,1}} \tag{4}$$

Thus,

$$\frac{dA}{dX} = \frac{\Delta V_N D \sin \Lambda}{V_{X,1}} \tag{5}$$

The following equation is obtained when equation (3) is substituted into equation (5):

$$\frac{dA}{dX} = \frac{V_{N,O}t \frac{D}{D - t} \sin \Lambda}{V_{X,1}} \tag{6}$$

and

$$\frac{dA}{dX} = \frac{V_O t \frac{D}{D - t}}{V_{X,1}} \sin \Lambda \cos \Lambda \tag{7}$$

Now let D become very large with respect to t; then

$$\frac{D}{D - t} \rightarrow 1$$

and

$$\frac{V_O}{V_{X,1}} \rightarrow 1$$

Thus,

$$\frac{dA}{dX} = t \sin \Lambda \cos \Lambda \tag{8}$$

For a wing that is tapered as well as swept, the variation in local sweep angle along the chord must also be considered. A graphical method for determination of the variation of area displacement along the chord for a tapered wing is presented in the appendix for the experimental models reported herein. The fuselage-modification method described by equation (8) will henceforth be referred to as the sine-cosine method in this report.

It is of interest to note that the sine-cosine method will at the most require only half as much area modification as that required by the area rule for a 45° sweptback untapered wing. There are also other dissimilarities. The sine-cosine modification is applicable only to sweptback wings and is specified only along the wing root chord. Also, the sine-cosine method specifies the variation of fuselage area along the root chord; whereas, the area rule specifies the fuselage area to be removed in order that a smooth equivalent body profile may be achieved.

MODELS

In order to investigate the effectiveness of the sine-cosine method, a flight test program was undertaken by the Langley Pilotless Aircraft Research Division. The general configuration chosen was the same as that used in a previous investigation (ref. 12) in order that comparisons could be made as to the relative effectiveness of the area-rule modifications.

The basic wing-body configuration had a wing swept at 45° along the 25-percent chord line, a taper ratio of 0.6, an aspect ratio of 4, and an NACA 65A004 airfoil section. The fuselage was a parabolic body of revolution with a fineness ratio of 12.5. The maximum diameter was at the 40-percent station and the ratio of the base diameter to maximum diameter was 0.5. This basic configuration will be designated as configuration A in this report. The basic configuration with the body indented according to the area rule for $M = 1$ and $M = 1.2$ will be designated as configurations B and C, respectively. These configurations have been previously tested and the results reported in reference 12.

The fuselage of configuration D was modified according to the sine-cosine method. This was accomplished in the following manner. From the nose to the leading edge of the wing root chord the body was identical to the basic body. Along the wing root chord the body cross-sectional area was determined by subtracting an area from the cross-sectional area of the body at the leading-edge station. The area to be subtracted was determined by graphical integration according to equation (8) but with allowance made for the effect of wing taper. The method of determining the area to be removed is outlined in the appendix. From approximately the trailing edge of the wing root chord to the base of the fuselage, the fuselage ordinates were determined by fairing in a parabolic curve. The maximum diameter of this parabolic afterbody was in the vicinity of the wing trailing edge and matched the minimum diameter specified by the body modification procedure; the base diameter was equal to that of the basic configuration. A three-view drawing of configuration D is shown in figure 1.

The fuselage of model E had the same cross-sectional-area variation along its length as model D but the cross-section shape was different, having been modified by flattening the sides in the vicinity of the wing. This modification was made in order that the sides of the fuselage would follow the same streamline contour as that specified in reference 9 for the streamline flow in the immediate vicinity of the wing surface. It should be noted that the wing plan form and airfoil used in this investigation are the same as that used in reference 9.

The fuselage of model F was identical to the fuselage of model D. Model F, however, had small bodies of revolution on the wing tips. These shapes, which will be referred to as tip stores, originated at the leading edge of the tip chord. The cross-sectional-area variation of the tip store along the tip chord was in accordance with the sine-cosine method. Behind the wing-tip trailing edge, the tip stores were faired to a pointed base with a parabolic curve. The tip stores had a fineness ratio of 11.6.

Table I presents the body ordinates for models D, E, and F; table II presents the ordinates of the wing-tip stores for model F; and table III presents the airfoil ordinates for the NACA 65A004 airfoil used on these configurations. Some details of the models tested may be noted in the photographs of the individual models. (See fig. 2.) Model F assembled on its booster and ready for launching is shown in a photograph taken at the launching site. (See fig. 3.)

A comparison of body contours is presented as a variation of body radius with station for models A, B, C, D, and F in figure 4(a). In figure 4(b) the body shape of model E is compared with that of models D and F. Models B and C had a body volume equal to 82 percent of that of model A, the basic model; whereas models D, E, and F had a body volume equal to 94 percent of that of model A. Model F had, in addition, the volume of its wing-tip stores which was equal to $3\frac{1}{4}$ percent of the basic body volume. It is uncertain, however, that the volume of these stores would always be valuable in practical applications.

TESTS AND MEASUREMENTS

All the models were tested at the Langley Pilotless Aircraft Research Station at Wallops Island, Va. They were propelled from zero-length launchers by fin-stabilized 5- by 65-inch rocket motors to supersonic speeds. After burnout of the rocket motors, the models drag-separated from the boosters and decelerated through the test Mach number range. Velocity and trajectory data were obtained from the CW Doppler velocimeter and NACA modified SCR-584 tracking radar unit, respectively. A survey of atmospheric conditions including winds aloft was made by rawinsonde measurements from an ascending balloon that was released at the time of each launching.

The flight tests covered a continuous range of Mach numbers which varied from approximately 0.9 to 1.35. The corresponding Reynolds numbers varied from approximately 3.0×10^6 to 5.75×10^6, based on wing mean aerodynamic chord, as is shown in figure 5.

The values of total drag coefficient, based on total wing planform area, were obtained during decelerating flight with the following expression:

$$C_D = -\frac{W}{qgS}(a + g \sin \gamma) \tag{9}$$

where a was obtained by differentiating the velocity time curve from the CW Doppler velocimeter. A more complete description of reducing the data is given in reference 13.

The probable error in total drag coefficient was estimated to be less than ±0.0007 at supersonic speeds and less than ±0.001 at subsonic speeds. The Mach numbers were determined within ±0.01 throughout the test range.

RESULTS AND DISCUSSION

Total Drag

The drag values obtained from the flight tests of models D, E, and F are presented in figure 6 as plots of drag coefficient against Mach number. Also shown in these figures is the friction drag coefficient which was arrived at in the following manner. It was assumed that all of the drag at $M = 0.9$ was due to friction; the resulting friction drag coefficient was then gradually reduced with increasing Mach number and Reynolds number at a rate that was determined from flat-plate theory.

It should be noted that model E, the configuration with the streamlined-contoured sides, had 20 percent more drag at subsonic speed than the other two models. Whereas this subsonic drag has been all attributed to friction, it may very easily have resulted from some other type of flow phenomenon such as vortex formations or separation at the fuselage corners. Similar large differences in subsonic drag level were previously reported in reference 8. However, in that case the circular-cross-section fuselage produced the highest drag.

It is also interesting to note that model F, the model with the tip stores, showed an unusually gradual drag rise. Although no reasonable explanation can be made for the shape of the drag-rise curve, the low drag level has been substantiated by theoretical calculations at speeds greater than $M = 1.07$.

Pressure Drag

In figure 7 the pressure drag coefficients for models D, E, and F are presented. Experimental pressure drag coefficients were obtained by subtracting the friction drag coefficient from the total drag coefficients shown in figure 6. Theoretical pressure drag coefficients were obtained using the calculation procedures of references 14 and 15. The theoretical drag calculations were carried out using 33 harmonics for the Fourier sine series solution. Since the body cross-sectional area was the same for models D and E, the theoretical drag is the same. However, above $M = 1.0$, the experimental pressure drag of model E was 10 to 20 percent less than that for model D. References 8 and 9 showed similar drag reductions resulting from contouring the fuselage sides to conform with the wing-surface streamline.

Fairly good agreement between theoretical and experimental pressure drag for the three models tested is indicated. Approximately the same agreement between experimental and theoretical results is shown in reference 12 for models A, B, and C.

Drag Comparison

In figure 8(a) experimental pressure drag coefficients of models D and F are compared with models A, B, and C of reference 12. A similar comparison of theoretical drag coefficients is shown in figure 8(b). Although the experimental drag curves were generally higher than the theoretical drag curves, the following comparative results may be obtained from either set of curves. The basic model (model A) had considerably higher pressure drag than any of the modified models. From $M = 1.15$ to $M = 1.3$, the $M = 1.0$ model (model B) had essentially the same drag as the sine-cosine model (model D) and the $M = 1.2$ model (model C) had essentially the same drag as the sine-cosine model with tip stores (model F). Furthermore, models B and D had considerably more drag than models C and F in this Mach number range. From $M = 1.0$ to 1.05, the $M = 1.2$ model (model C) and the sine-cosine model (model D) had close to the same drag.

The sine-cosine modification without the tip stores (model D) appears to be the least effective of the body modifications in reducing the drag over the entire Mach number range. However, the sine-cosine body modifications reduced the volume of the basic body by only 6 percent as compared to 18-percent reduction for the area-rule modification (models B and C). An adjustment in frontal area to equalize the volume would quite likely also equalize the drag values.

The sine-cosine model with the tip stores (model F) proved to be the best all-around design. It had the least drag or nearly the least

drag at all Mach numbers. Since it only had a 6-percent decrease in fuselage volume as compared to the basic body, it would show up even better if a volume adjustment had been made. In addition, the volume of the tip stores ($3\frac{1}{4}$ percent of the basic body volume) is obtained as a byproduct of the modification.

By comparing model D (sine-cosine) with model F (sine-cosine plus stores), it can be seen that the addition of the tip stores resulted in an appreciable reduction in the pressure drag. An area-rule explanation for this may be found in that the addition of the store lengthens the bump caused by the wing on the area diagram (fig. 9). However, it should be pointed out that the store does not completely "correct" the area distribution and the resulting area diagram is not nearly as smooth or ideal as that of model B. Pressure-drag benefits from stores located in a rearward position on the wing tip were also reported in reference 16. A theoretical basis for the concept of employing auxiliary bodies along the wing was developed in reference 17. Thus, it can be seen that the proposal to use stores for drag reduction is neither new nor in conflict with existing theory.

It should be apparent that there is a basic difference in the area-rule modification and the sine-cosine modification. In the usual case of area-rule modifications, the interference drag from the wing in the region of the wing tip, as well as the wing root region, is reduced by fuselage modifications. The sine-cosine modification is applicable only to sweptback wings and attempts to reduce only the wing-root interference by fuselage shaping; reduction of wing-tip interference is accomplished at the wing tip with a specifically shaped store. The advantage of the use of wing-tip stores is apparent when it is considered that pressure fields emanating from fuselage shapes are partially dissipated out at the wing tip and are properly located only at one Mach number.

Since area-rule analysis was used to make theoretical pressure drag calculations which showed the sine-cosine method to be very effective, the sine-cosine method obviously is not in disagreement with the area rule. The sine-cosine method, however, offers an alternate design procedure when low drag is desired over a fairly wide Mach number range.

CONCLUDING REMARKS

A method for reducing the interference pressure drag of the root and tip of sweptback wings has been developed. Models designed by this method have been compared experimentally and theoretically with models designed by the transonic and supersonic area-rule method. These comparisons were made useing a 45° sweptback-wing configuration over the

speed range from Mach number 0.9 to 1.35. The main results of this investigation are as follows:

1. Experimental and theoretical results were in general agreement in that both indicated the same relative order of drag levels for the various configurations.

2. All modifications to the basic configuration effected considerable reductions in pressure drag.

3. The area-rule modifications were better than the sine-cosine modifications without tip stores in reducing pressure drag. However, the area-rule modifications required a volume reduction of 18 percent of the basic fuselage volume as compared to a reduction of only 6 percent for the sine-cosine modification.

4. The sine-cosine modification with tip stores was better than the transonic area-rule modification and equal to the supersonic area-rule modification in reducing the drag over the Mach number range. A volume adjustment to the sine-cosine configuration with tip stores would make this configuration better than the supersonic area-rule configuration.

Langley Aeronautical Laboratory,
National Advisory Committee for Aeronautics,
Langley Field, Va., April 5, 1957.

APPENDIX

GRAPHICAL METHOD USED FOR TAPERED WINGS

Equation (8) was derived for an untapered wing. In applying this equation to the case of a tapered wing, the wing may be treated as a succession of slightly tapered spanwise strips, each strip having a different sweep angle. If the strips are made small enough, there is essentially no difference in the sweep angle of the leading edge and trailing edge of the strip. Each strip is treated as if it were of triangular cross section with the difference in thickness between leading edge and trailing edge of the strip used as the height of the triangle. Thus the change in $\frac{dA}{dX}$ from the leading edge to the trailing edge of the strip is proportional to the change in thickness, and the following equation is obtained:

$$\frac{d^2A}{dX^2} = \frac{dt}{dX} \sin \Lambda \cos \Lambda = \frac{dt}{dX}\left(\frac{\tan \Lambda}{\tan^2 \Lambda + 1}\right) \tag{10}$$

Inasmuch as the thickness variation of most airfoils may not be given in equation form, the double integration must be carried out graphically. This was done for the wing used in this report by using the following procedure.

The wing was first laid out in 10 strips as shown in the following sketch:

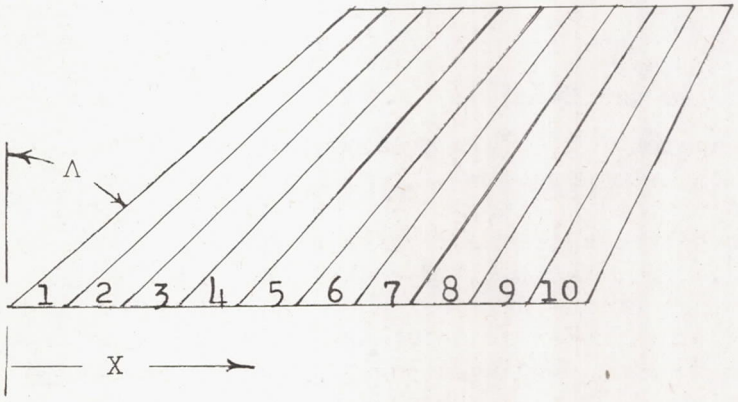

The average slope of each strip is determined along with the change in thickness across the strip. Since there are two wings, twice the

change in thickness is used in the calculations. The calculation of $\frac{dA}{dX}$ is carried out for the root chord as follows:

X, in.	t (one wing), in.	Strip	Δt (two wings), in.	Average slope, tan Λ	$\frac{\tan \Lambda}{\tan^2 \Lambda + 1}$	$\frac{d^2A}{dX^2}$	$\frac{dA}{dX}$
0	0						
		1	0.412	1.05	0.4994	0.2057	
.85	.206						0.2057
		2	.148	1.025	.4999	.0740	
1.70	.280						.2797
		3	.084	1.00	.5000	.0420	
2.55	.322						.3217
		4	.034	.975	.4998	.0170	
3.40	.339						.3387
		5	-.014	.95	.4993	-.0070	
4.25	.332						.3317
		6	-.072	.925	.4985	.0359	
5.10	.296						.2958
		7	-.116	.900	.4972	.0577	
5.95	.238						.2381
		8	-.148	.875	.4956	.0733	
6.80	.164						.1648
		9	-.162	.85	.4935	.0799	
7.65	.083						.0849
		10	-.162	.825	.4909	.0795	
8.50	.002						.0054

Then, $\frac{dA}{dX}$ is plotted against X. The resulting curve is then integrated to determine the variation of A with X. In figure 10, $\frac{dA}{dX}$ and A are plotted against X. This area is subtracted from the area of the fuselage at the wing-root leading edge to determine the fuselage area along the root chord. Inasmuch as the tapering of the fuselage exposed additional wing cross-sectional area between the fuselage and the root chord extended from the leading-edge—fuselage juncture, a small correction in fuselage cross-sectional area was included. The cross-sectional area for the tip stores was determined from the wing-root calculations by geometric scaling, the area being proportional to the square of the ratio of tip chord to root chord.

REFERENCES

1. Küchemann, D.: Design of Wing Junction, Fuselage, and Nacelles To Obtain the Full Benefit of Sweptback Wings at High Mach Number. Rep. No. Aero. 2219, British R.A.E., Aug. 1947.

2. Watkins, Charles E.: The Streamline Pattern in the Vicinity of an Oblique Airfoil. NACA TN 1231, 1947.

3. McDevitt, John B.: An Experimental Investigation of Two Methods for Reducing Transonic Drag of Swept-Wings and Body Combinations. NACA RM A55D21, 1955.

4. McDevitt, John B., and Haire, William M.: Investigation at High Subsonic Speeds of a Body-Contouring Method for Alleviating the Adverse Interference at the Root of a Sweptback Wing. NACA TN 3672, 1956. (Supersedes NACA RM A54A22.)

5. Boddy, Lee E.: Investigation at High Subsonic Speeds of Methods of Alleviating the Adverse Interference at the Root of a Swept-Back Wing. NACA RM A50E26, 1950.

6. Hartley, D. E.: Investigation at High Subsonic Speeds of Wing-Fuselage Interference Shapes for Sweptback Wings. Part I. Force Measurements on Some Initial Designs. Rep. No. Aero. 2464, British R.A.E., May 1952.

7. Pepper, William B.: The Effect on Zero-Lift Drag of an Indented Fuselage or a Thickened Wing-Root Modification to a 45° Sweptback Wing-Body Configuration As Determined by Flight Tests at Transonic Speeds. NACA RM L51F15, 1951.

8. Howell, Robert R., and Braslow, Albert L.: An Experimental Study of a Method of Designing the Sweptback-Wing—Fuselage Juncture for Reducing the Drag at Transonic Speeds. NACA RM L54L31a, 1955.

9. Howell, Robert R.: Experimental Study of a Method of Designing the Sweptback-Wing—Fuselage Juncture To Reduce the Drag at Moderate Supersonic Speeds. NACA RM L55H05a, 1956.

10. Palmer, William E., Howell, Robert R., and Braslow, Albert L.: Transonic Investigation at Lifting Conditions of Streamline Contouring in the Sweptback-Wing—Fuselage Juncture in Combination With the Transonic Area Rule. NACA RM L56D11a, 1956.

11. Whitcomb, Richard T.: A Study of the Zero-Lift Drag-Rise Characteristics of Wing-Body Combinations Near the Speed of Sound. NACA Rep. 1273, 1956. (Supersedes NACA RM L52H08.)

12. Blanchard, Willard S., Jr., and Hoffman, Sherwood: A Flight Investigation To Determine the Effectiveness of Mach Number 1.0, 1.2, and 1.41 Fuselage Indentations for Reducing the Pressure Drag of a 45° Sweptback Wing Configuration at Transonic and Low Supersonic Speeds. NACA RM L57B27, 1957.

13. Wallskog, Harvey A., and Hart, Roger G.: Investigation of the Drag of Blunt-Nosed Bodies of Revolution in Free Flight at Mach Numbers From 0.6 to 2.3. NACA RM L53D14a, 1953.

14. Holdaway, George H.: Comparison of Theoretical and Experimental Zero-Lift Drag-Rise Characteristics of Wing-Body-Tail Combinations Near the Speed of Sound. NACA RM A53H17, 1953.

15. Alksne, Alberta: A Comparison of Two Methods for Computing the Wave Drag of Wing-Body Combinations. NACA RM A55A06a, 1955.

16. Pepper, William B., Jr., and Hoffman, Sherwood: Comparison of Zero-Lift Drag Determined by Flight Tests at Transonic Speeds of Symmetrically Mounted Nacelles in Various Chordwise Positions at the Wing Tip of a 45° Sweptback Wing and Body Combination. NACA RM L51F13, 1951.

17. Baldwin, Barrett, Jr., and Dickey, Robert R.: Application of Wing-Body Theory to Drag Reduction at Low Supersonic Speeds. NACA RM A54J19, 1955.

TABLE I

FUSELAGE ORDINATES FOR MODELS D, E, AND F

Station, in.	Radius of models D and F, in.	Radius of model E, in.	Width of model E, in.
0	0	0	0
1	.194	.194	.194
2	.315	.315	.315
3	.544	.544	.544
4	.700	.700	.700
5	.844	.844	.844
6	.975	.975	.975
7	1.094	1.094	1.094
8	1.200	1.200	1.200
9	1.296	1.296	1.296
10	1.373	1.373	1.373
11	1.444	1.444	1.444
12	1.500	1.500	1.500
13	1.544	1.544	1.544
14	1.575	1.575	1.575
15	1.594	1.594	1.594
16	1.600	1.600	1.600
17	1.583	1.586	1.539
18	1.554	1.563	1.468
19	1.518	1.534	1.393
20	1.479	1.508	1.315
21	1.444	1.490	1.239
22	1.412	1.482	1.181
23	1.393	1.484	1.143
24	1.384	1.485	1.130
25	1.376	1.475	1.130
26	1.363	1.455	1.130
27	1.346	1.427	1.130
28	1.326	1.395	1.130
29	1.302	1.358	1.130
30	1.275	1.316	1.130
31	1.244	1.271	1.130
32	1.209	1.224	1.130
33	1.171	1.177	1.127
34	1.129	1.130	1.114
35	1.083	1.083	1.083
36	1.034	1.034	1.034
37	.981	.981	.981
38	.924	.924	.924
39	.864	.864	.864
40	.800	.800	.800

TABLE II

WING-TIP STORE ORDINATES

FOR MODEL F

Station, in.	Radius, in.
0	0
.6	.111
1.2	.189
1.8	.243
2.4	.288
3.0	.322
3.6	.343
4.2	.355
4.8	.358
5.4	.354
6.0	.342
6.6	.321
7.2	.290
7.8	.255
8.4	.210
9.0	.157
9.6	.095
10.4	0

TABLE III

COORDINATES OF NACA 65A004 AIRFOIL

[Stations measured from leading edge]

Station, percent chord	Ordinate, percent chord
0	0
.5	.311
.75	.378
1.25	.481
2.5	.656
5.0	.877
7.5	1.062
10	1.216
15	1.463
20	1.649
25	1.790
30	1.894
35	1.962
40	1.996
45	1.996
50	1.952
55	1.867
60	1.742
65	1.584
70	1.400
75	1.193
80	.966
85	.728
90	.490
95	.249
100	.009
L.E. radius: 0.102 percent chord T.E. radius: 0.010 percent chord	

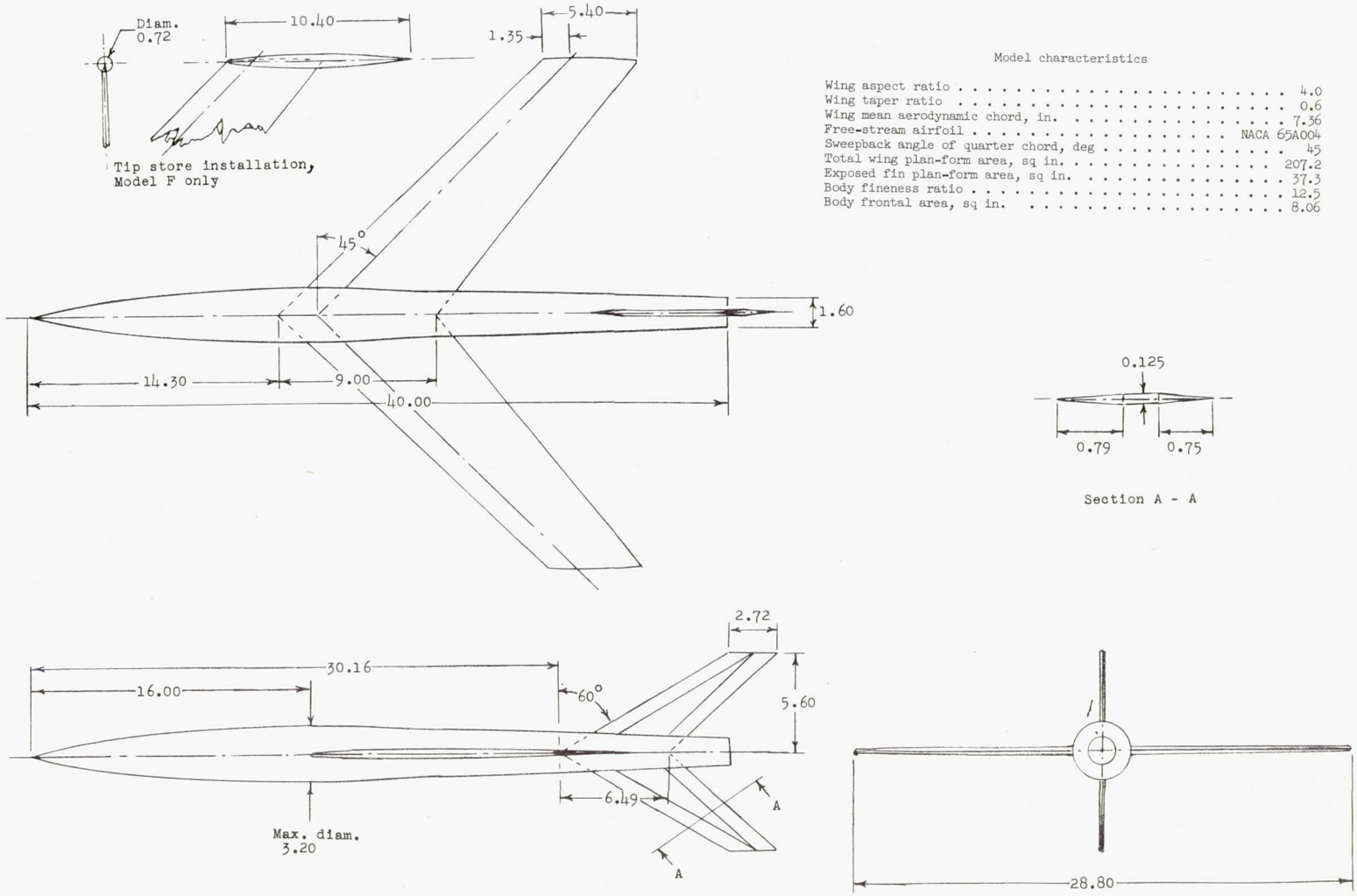

Model characteristics

Wing aspect ratio	4.0
Wing taper ratio	0.6
Wing mean aerodynamic chord, in.	7.36
Free-stream airfoil	NACA 65A004
Sweepback angle of quarter chord, deg	45
Total wing plan-form area, sq in.	207.2
Exposed fin plan-form area, sq in.	37.3
Body fineness ratio	12.5
Body frontal area, sq in.	8.06

Figure 1.- General details and dimensions of configuration D. All dimensions are in inches.

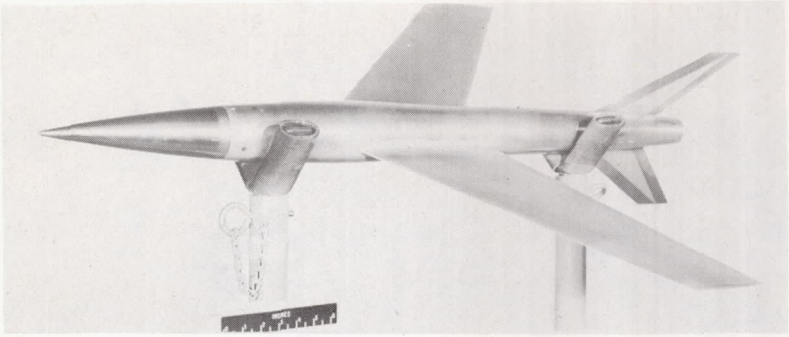

(a) Model D with sine-cosine indentation.

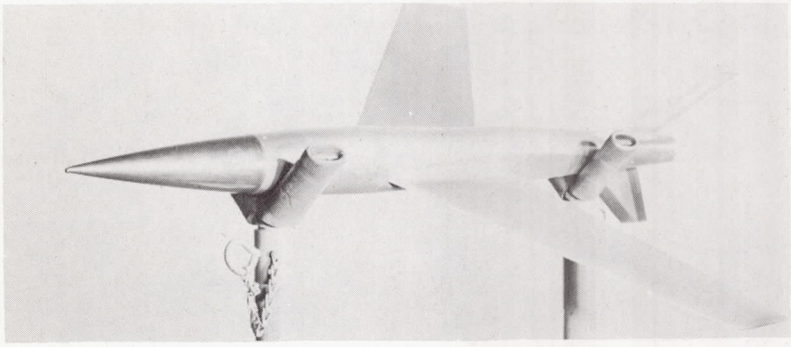

(b) Model E with streamline-contoured sides.

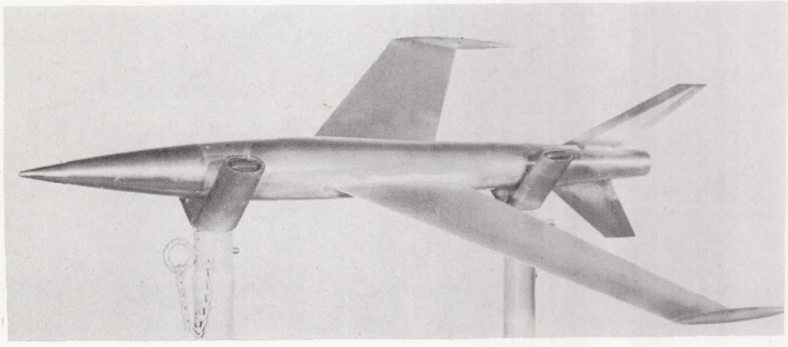

L-57-1555

(c) Model F with sine-cosine indentation and wing-tip stores.

Figure 2.- Photographs of configurations tested.

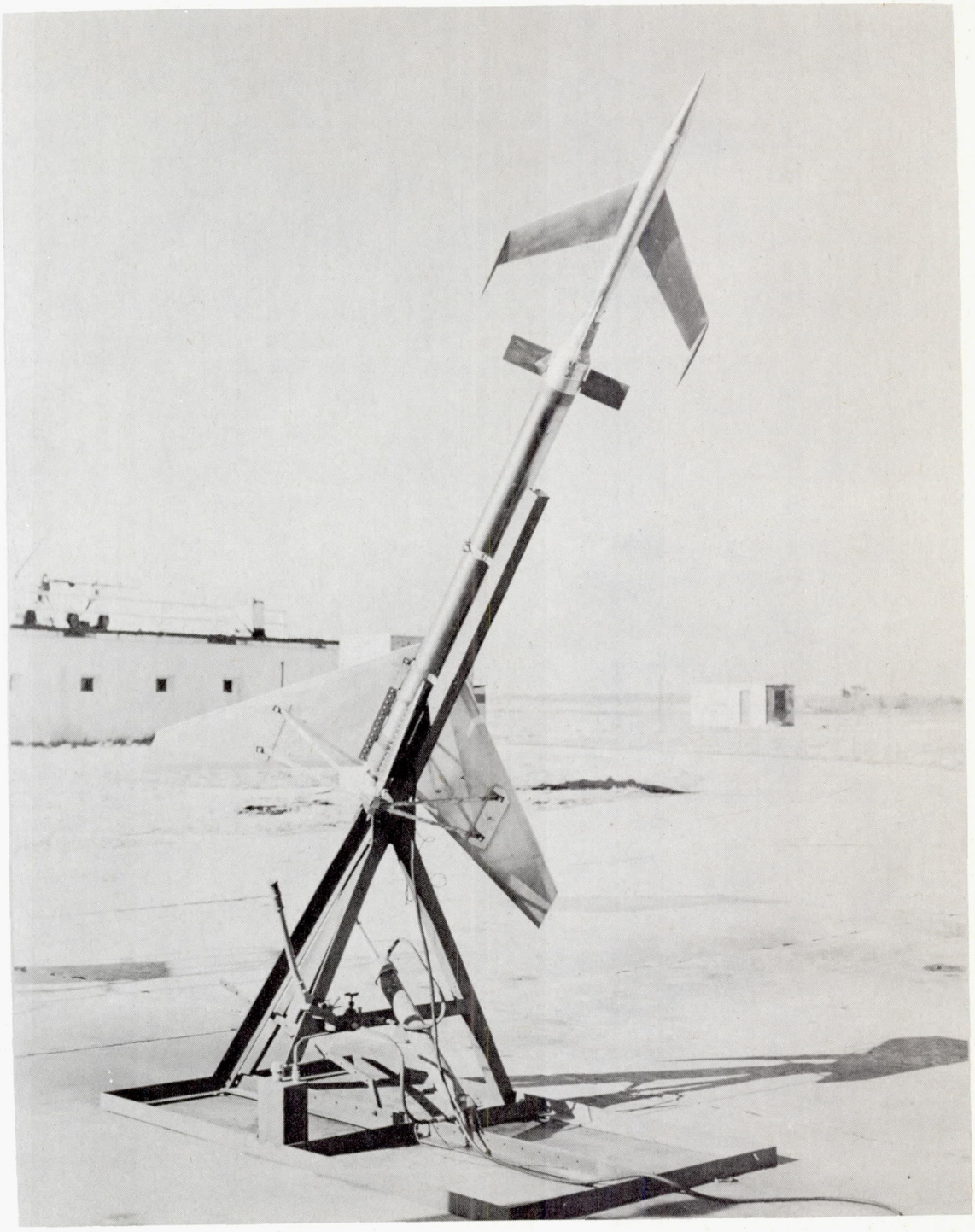

Figure 3.- Photograph of model F and booster on launcher. L-93084.1

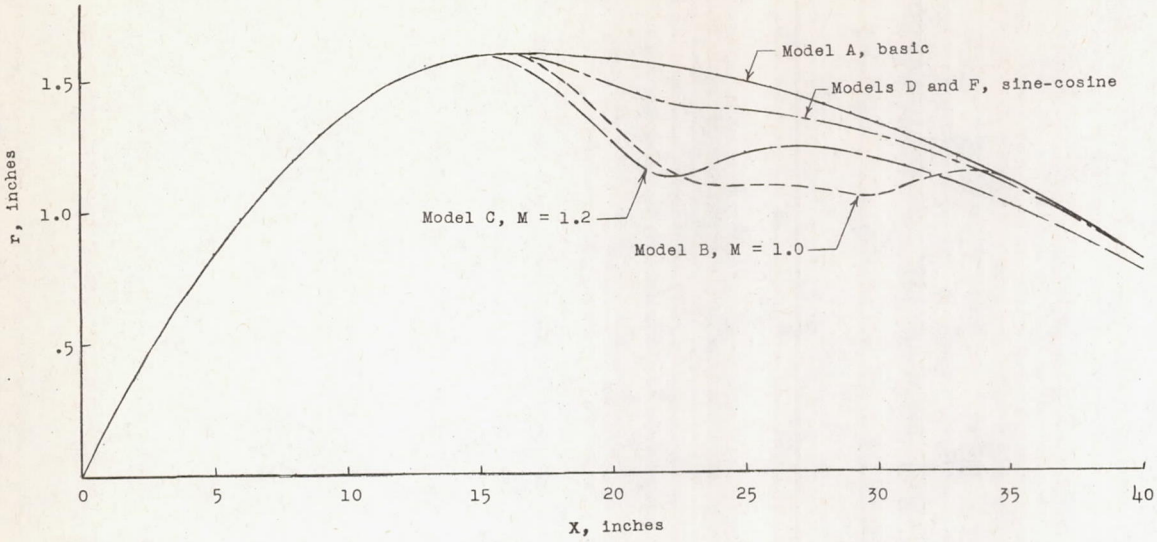

(a) Body-radius variation of models D and F compared with that of models A, B, and C from reference 12.

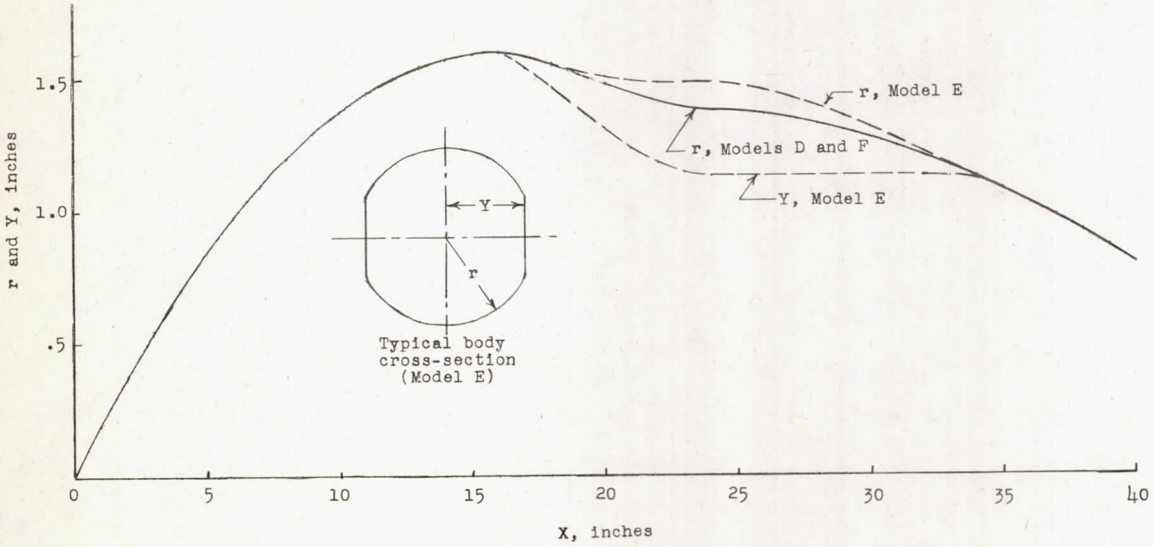

(b) Cross-section shape of model E compared with circular cross section of models D and F. (Equal cross-sectional areas at all stations.)

Figure 4.- Comparison of body shapes.

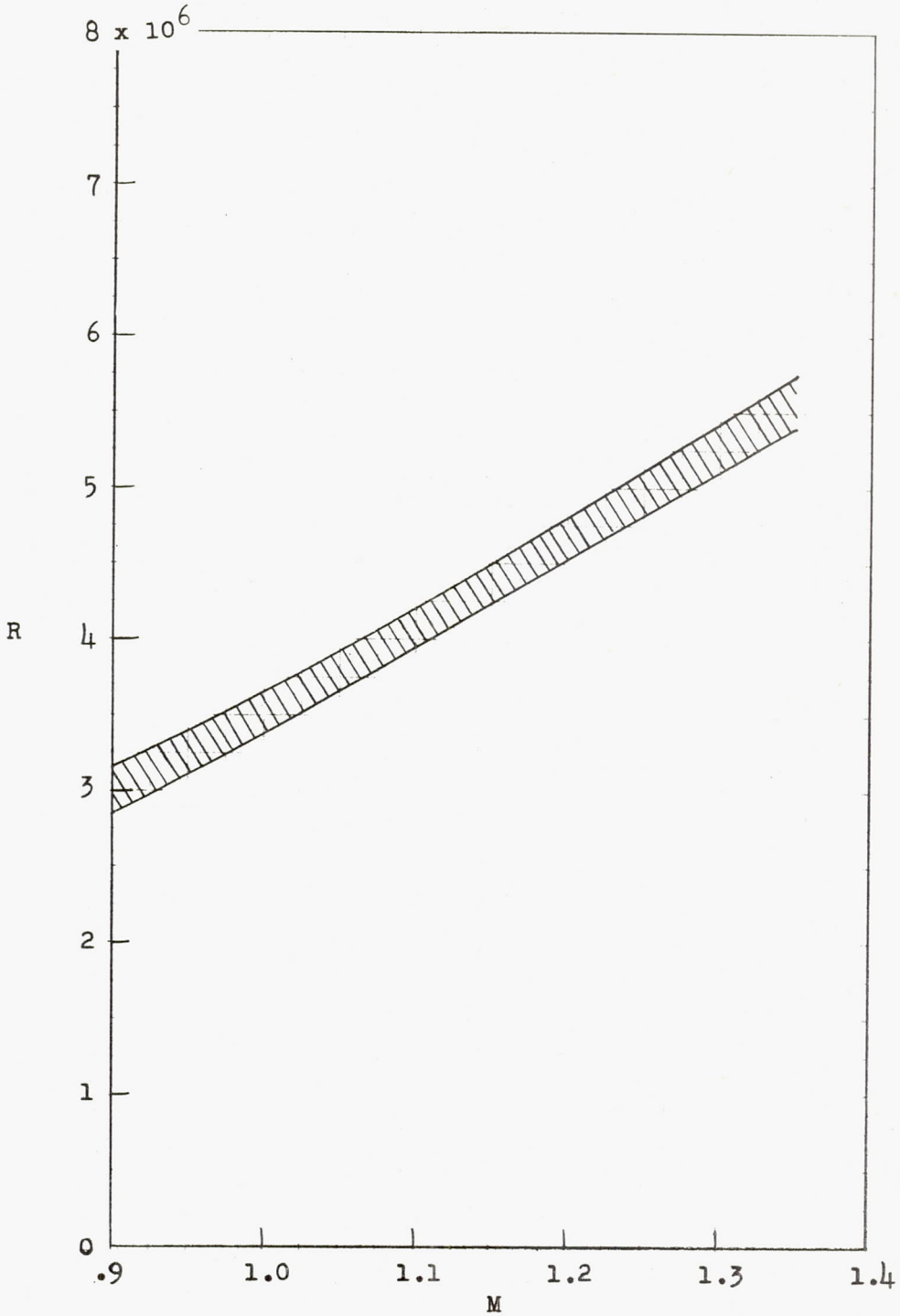

Figure 5.- Variation of Reynolds number with Mach number for models tested. Reynolds number is based on wing mean aerodynamic chord.

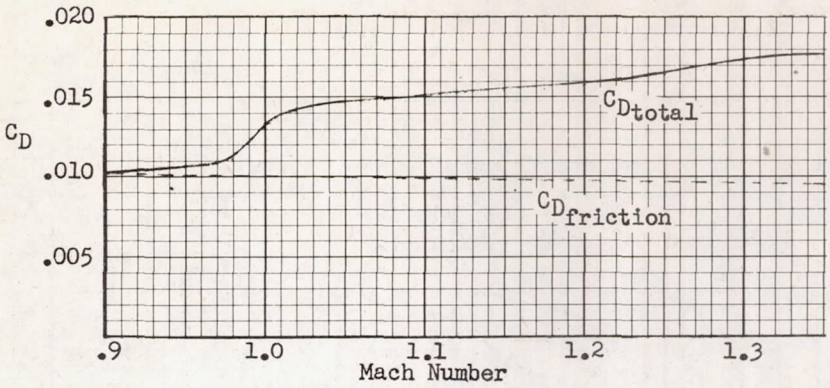

(a) Model D (sine-cosine with circular cross section).

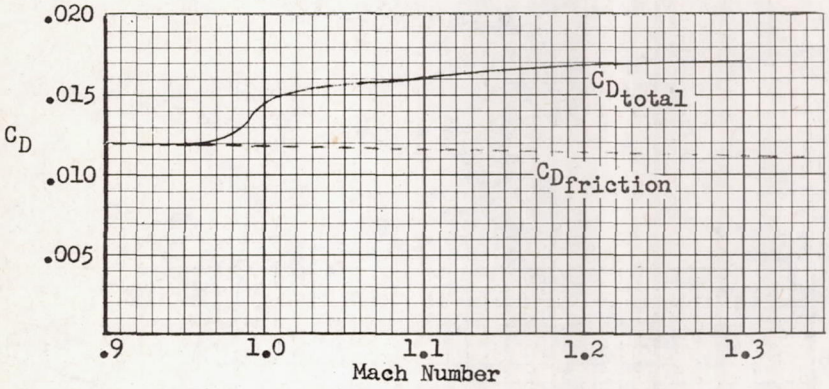

(b) Model E (sine-cosine with streamline-contoured sides).

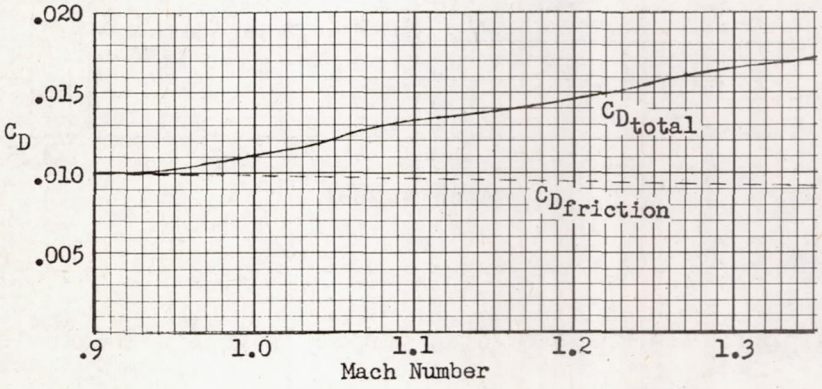

(c) Model F (sine-cosine plus wing-tip stores).

Figure 6.- Drag coefficients for models tested.

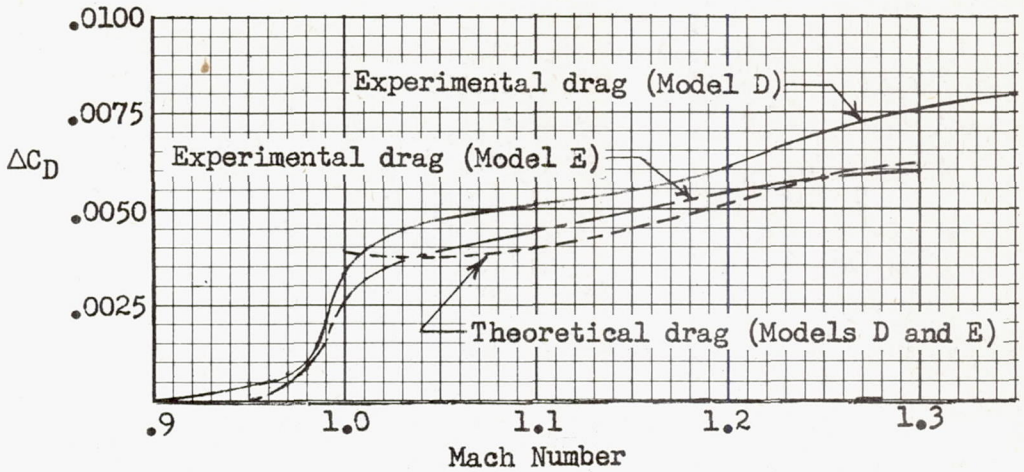

(a) Model D (sine-cosine with circular cross section) and model E (sine-cosine with streamline-contoured sides).

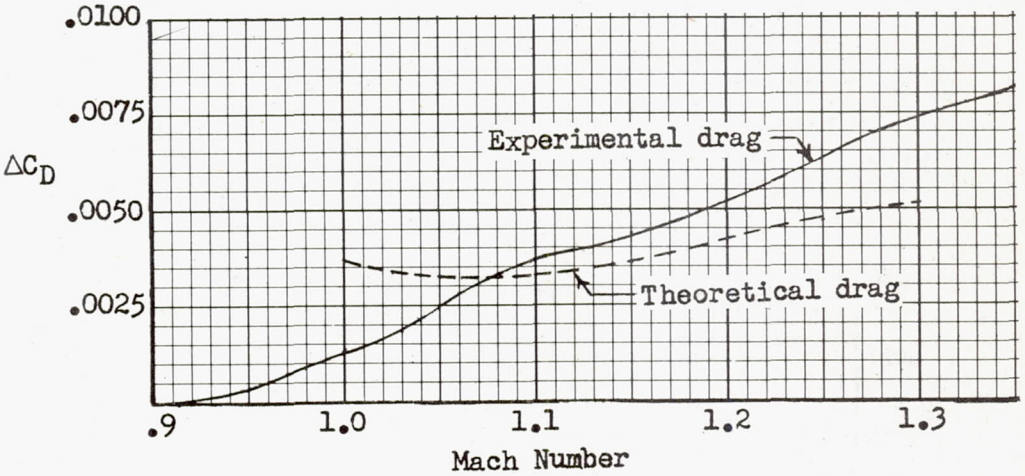

(b) Model F (sine-cosine plus wing-tip stores).

Figure 7.- Pressure-drag coefficients for models tested.

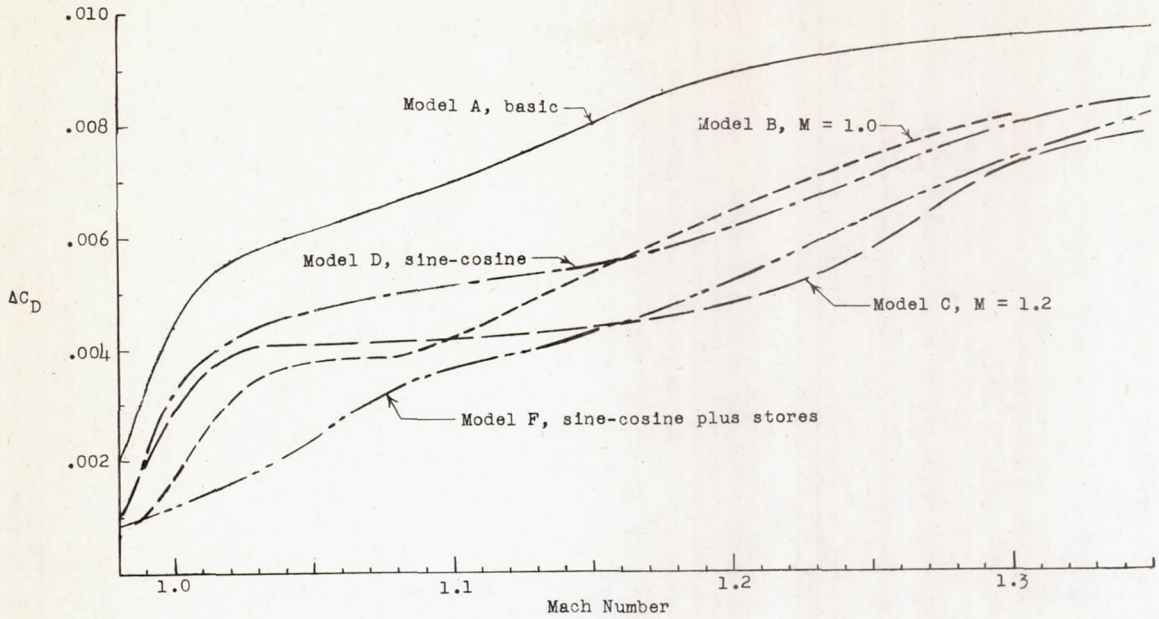

(a) Experimental pressure-drag coefficients.

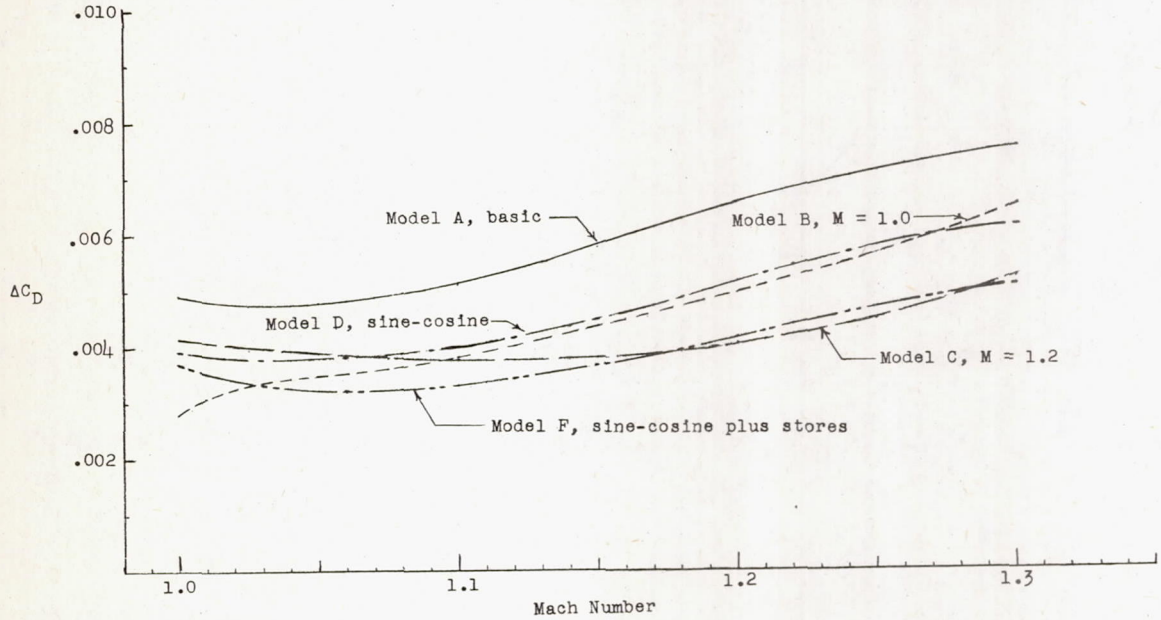

(b) Theoretical pressure-drag coefficients.

Figure 8.- Comparison of pressure-drag coefficients.

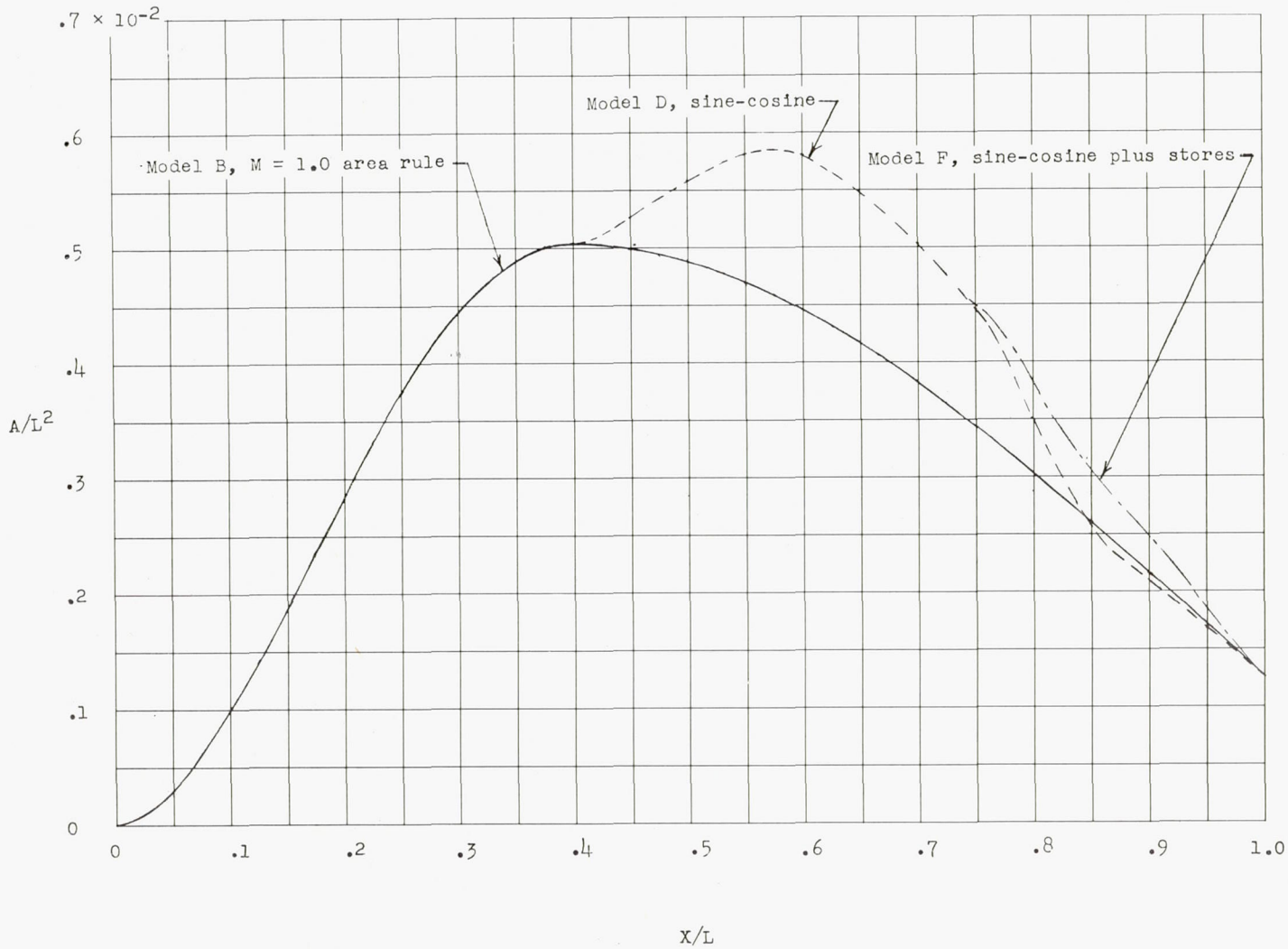

Figure 9.- Normal-cross-sectional-area distribution of models tested compared with model B, the M = 1.0 area-rule configuration.

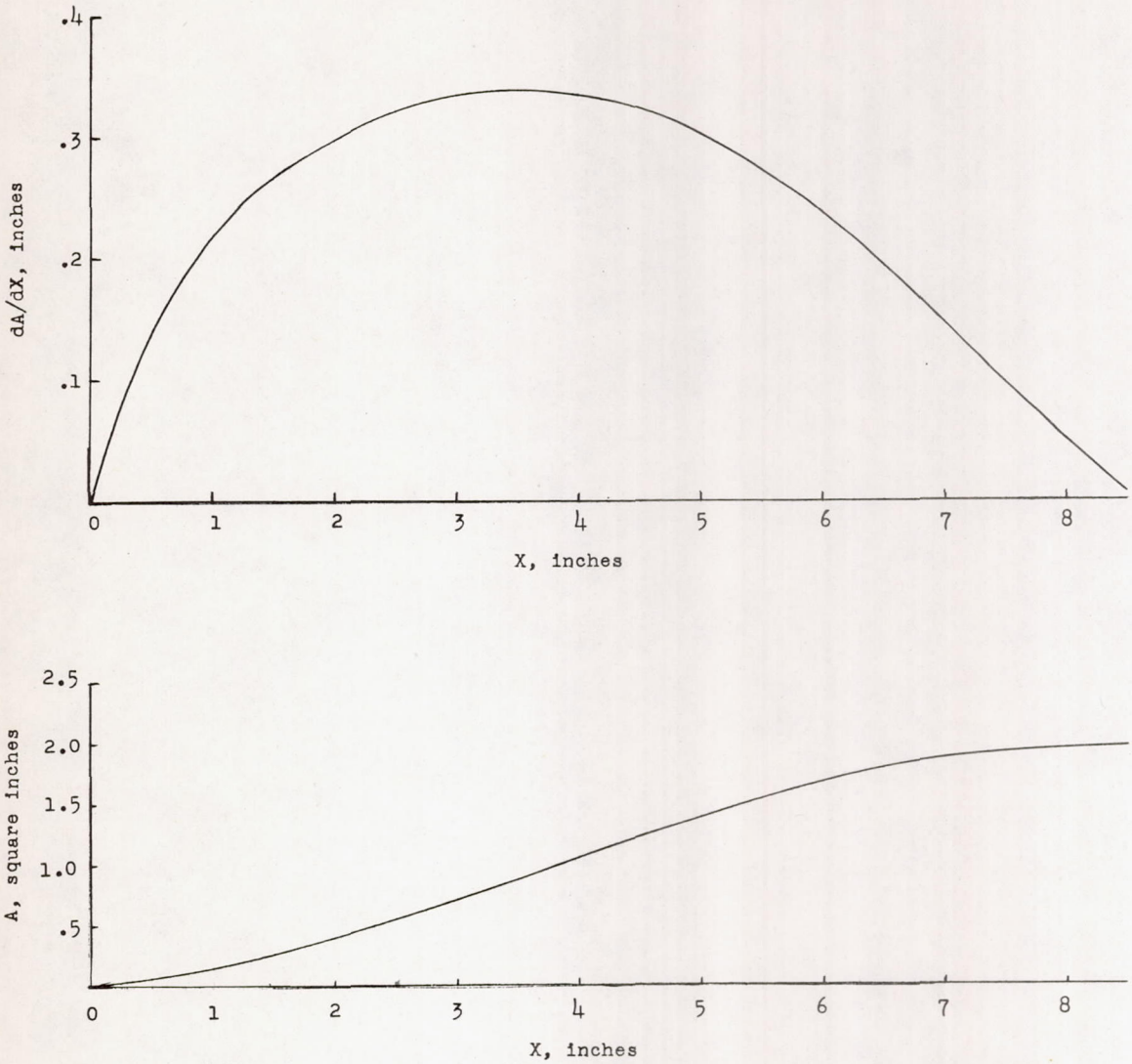

Figure 10.- Plot of dA/dX and A against X for determination of variation of body cross-sectional area.